# Characterization of the functional role of allosteric site residue Asp$^{102}$ in the regulatory mechanism of human mitochondrial NAD(P)$^+$-dependent malate dehydrogenase (malic enzyme)

Hui-Chih HUNG*[1], Meng-Wei KUO*, Gu-Gang CHANG† and Guang-Yaw LIU‡[1]

*Department of Life Sciences, National Chung-Hsing University, Taichung 402, Taiwan, Republic of China, †Faculty of Life Sciences, Institute of Biochemistry, and Structural Biology Program, National Yang-Ming University, Taipei 112, Taiwan, Republic of China, and ‡Institute of Immunology, Chung-Shan Medical University, Taichung 402, Taiwan, Republic of China

Human mitochondrial NAD(P)$^+$-dependent malate dehydrogenase (decarboxylating) (malic enzyme) can be specifically and allosterically activated by fumarate. X-ray crystal structures have revealed conformational changes in the enzyme in the absence and in the presence of fumarate. Previous studies have indicated that fumarate is bound to the allosteric pocket via Arg$^{67}$ and Arg$^{91}$. Mutation of these residues almost abolishes the activating effect of fumarate. However, these amino acid residues are conserved in some enzymes that are not activated by fumarate, suggesting that there may be additional factors controlling the activation mechanism. In the present study, we tried to delineate the detailed molecular mechanism of activation of the enzyme by fumarate. Site-directed mutagenesis was used to replace Asp$^{102}$, which is one of the charged amino acids in the fumarate binding pocket and is not conserved in other decarboxylating malate dehydrogenases. In order to explore the charge effect of this residue, Asp$^{102}$ was replaced by alanine, glutamate or lysine. Our experimental data clearly indicate the importance of Asp$^{102}$ for activation by fumarate. Mutation of Asp$^{102}$ to Ala or Lys significantly attenuated the activating effect of fumarate on the enzyme. Kinetic parameters indicate that the effect of fumarate was mainly to decrease the $K_m$ values for malate, $Mg^{2+}$ and $NAD^+$, but it did not notably elevate $k_{cat}$. The apparent substrate $K_m$ values were reduced by increasing concentrations of fumarate. Furthermore, the greatest effect of fumarate activation was apparent at low malate, $Mg^{2+}$ or $NAD^+$ concentrations. The $K_{act}$ values were reduced with increasing concentrations of malate, $Mg^{2+}$ and $NAD^+$. The Asp$^{102}$ mutants, however, are much less sensitive to regulation by fumarate. Mutation of Asp$^{102}$ leads to the desensitization of the co-operative effect between fumarate and substrates of the enzyme.

Key words: allosteric activation, fumarate, malate dehydrogenase, malic enzyme, mutagenesis, enzyme regulation.

## INTRODUCTION

MDH [malate dehydrogenase (decarboxylating); malic enzyme; EC 1.1.1.39] is a homotetrameric enzyme with a double dimer quaternary structure that catalyses the bivalent metal ion ($Mn^{2+}$ or $Mg^{2+}$)-dependent reversible oxidative decarboxylation of L-malate to yield $CO_2$ and pyruvate, with concomitant reduction of NAD(P)$^+$ to NAD(P)H [1–5]. The enzymes are widely distributed in Nature, with conserved sequences and similar overall structural topology among different species ([6–9]; see [10] for a review). In mammals, based on their nucleotide specificity, the enzymes are grouped into three isoforms: cytosolic NADP$^+$-dependent (c-NADP-MDH), mitochondrial NADP$^+$-dependent (m-NADP-MDH), and mitochondrial NAD(P)$^+$-dependent (m-NAD-MDH) MDHs [11]. It has been shown that m-NAD-MDH can use either $NAD^+$ or $NADP^+$ as a cofactor, but prefers $NAD^+$ under physiological conditions [3].

In tumour cells, glutamine and glutamate, rather than glucose, are the major energy sources [13,14]. Human m-NAD-MDH, via the NADH and pyruvate products, is considered to have an important role in the metabolism of glutamate in rapidly proliferating tissues, particularly in tumour cells [3,12,13,15–18]. Thus the possible involvement of m-NAD-MDH in neoplasia has attracted much attention. m-NAD-MDH is distinct from the other two mammalian isoforms in that it shows co-operative behaviour with respect to the substrate malate, as well as being an allosteric enzyme, which is activated by fumarate and inhibited by ATP [1,3,16,19]. The allosteric properties of this enzyme isoform are integrated into a rationale for its specific role in the pathways of malate and glutamine oxidation in tumour cell mitochondria [17,19].

Various crystal structures of the enzyme in complexes with substrate, metal ion, cofactor, regulator and inhibitor have been successfully resolved since 1999 [6–9,20–22]. There are a total of 14 crystal structures available in the Protein Data Bank. From the structural information, the enzymes are suggested to belong to a new class of oxidative decarboxylases [6,10]. The availability of these structures opens up a new avenue of research on the structure–function relationship of this important enzyme.

The catalytic activity of m-NAD-MDHs from both human and *Ascaris suum* is activated by fumarate [19,23–25], and the binding site for fumarate in human m-NAD-MDH has been identified [20]. In the *A. suum* m-NAD-MDH, the same position is occupied by a tartronate molecule, which could represent a comparable allosteric binding site [21]. Figure 1(A) shows the fumarate binding site at the dimer interface, which is approx. 30 Å (3 nm) from the active site, verifying that fumarate operates through an allosteric mechanism [20]. Structural and kinetic studies have revealed that Arg$^{67}$ and Arg$^{91}$ are essential amino acid residues for activation of the enzyme by fumarate. One carboxylate group of fumarate has bidentate ion-pair interactions with the side chain of Arg$^{91}$, whereas the other is in a monodentate ion pair with Arg$^{67}$

Abbreviations used: MDH, malate dehydrogenase (malic enzyme); c-NADP-MDH, cytosolic NADP$^+$-dependent MDH; m-NADP-MDH, mitochondrial NADP$^+$-dependent MDH; m-NAD-MDH, mitochondrial NAD(P)$^+$-dependent MDH; WT, wild type.

[1] To whom correspondence should be addressed (email hchung@dragon.nchu.edu.tw or email liugy@csmu.edu.tw).

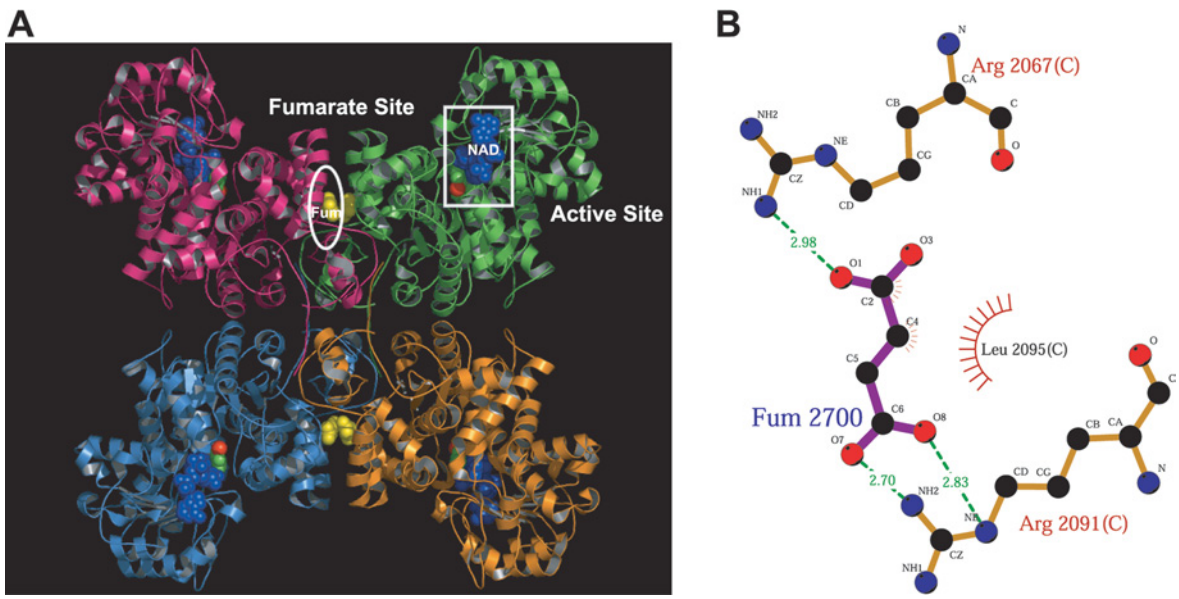


**Figure 1 Crystal structure and fumarate binding pocket of human m-NAD-MDH**

(**A**) Crystal structure of the enzyme in complex with $NAD^+$, pyruvate, $Mn^{2+}$ and fumarate (PDB code 1pj3). The active- and fumarate-site regions are highlighted with white boxes. Blue denotes $NAD^+$, green denotes pyruvate, and red denotes $Mn^{2+}$ in the active site; yellow denotes fumarate in the dimer interface. This figure was generated with PyMOL (DeLano Scientific LLC, San Carlos, CA, U.S.A.). (**B**) Fumarate binding ligands of human m-NAD-MDH are shown as a LIGPLOT diagram [29]. The bold bonds belong to the fumarate, the thin bonds belong to the hydrogen-bonded residues from the enzyme, and the dashed lines represent the hydrogen bonds. Spoked arcs represent hydrophobic contacts.

(Figure 1B). Mutation of $Arg^{67}$ and $Arg^{91}$ of human m-NAD-MDH leads to desensitization of the enzyme towards fumarate, confirming the importance of these residues in fumarate binding [20]. Both residues are conserved in *A. suum* m-NAD-MDH, as well as among many other decarboxylating MDHs that are insensitive to fumarate. Therefore additional amino acid residues may be involved in the mechanism of activation by fumarate in the m-NAD-MDHs from human and *A. suum* [20,25].

Here we report a detailed kinetic analysis of the activation of human m-NAD-MDH by fumarate. We further explore the functional role of the anionic residue $Asp^{102}$ in fumarate activation. We suggest that $Asp^{102}$ is an essential residue in the mechanism of activation by fumarate, due to its contribution to the charge balance with other charged residues in the allosteric site of human m-NAD-MDH.

## MATERIALS AND METHODS

### Expression and purification of recombinant human m-NAD-MDH

The expression and purification steps were modified from earlier protocols [3,26]. m-NAD-MDH was overexpressed in *Escherichia coli* BL21 cells in the expression vector pRH281 under the control of the inducible trp promoter system [3], and purified by anion-exchange chromatography on DEAE-Sepharose (Amersham Biosciences), followed by ATP–agarose affinity chromatography (Sigma). The purified enzymes were exchanged and concentrated using a Centricon 30 000 instrument (Amicon) with 30 mM Tris/HCl (pH 7.4). The enzyme purity was examined by SDS/PAGE, and protein concentrations were determined by the Bradford method [27].

### Site-directed mutagenesis

Site-directed mutagenesis was carried out using the QuikChange™ kit (Stratagene). This mutagenesis method was performed using Pfu DNA polymerase, which replicated both plasmid strands with high fidelity in a 16–20-cycle PCR reaction. Primers including the mutation site are 25–45 mers, which is required for specific binding of template DNA. The synthetic oligonucleotides used as mutagenic primers were 5′ GAATACTGCAAGCTGACATTGAGAGTTTAATGCC 3′ for D102A, 5′ GAATACTGCAAGAAGACATTGAGAGTTTAATGCC 3′ for D102E, and 5′ GTTTTATAGAATACTGCAAAAAGACATTGAGAGTTTAATGCC 3′ for D102K (mutation positions are underlined). After completing the mutagenic reactions, plasmid constructs were sequenced to confirm the presence of the desired mutations.

### Enzyme kinetics

For the m-NAD-MDH activity assay, the reaction mixture contained 50 mM Tris/HCl (pH 7.4), 15 mM malate (pH 7.4), 1.0 mM $NAD^+$ and 10 mM $MgCl_2$ in a total volume of 1 ml. After the enzyme was added to the reaction mixture, the absorbance at 340 nm at 30 °C was traced continuously in a Beckman DU 7500 spectrophotometer. In this process, one enzyme unit was defined as the amount of enzyme that can catalyse the production of 1 $\mu$mol of NADH per min. An absorption coefficient of 6220 $M^{-1}$ for NADH was used in calculations. Apparent Michaelis constants for the substrate and cofactors were determined by varying the concentration of one substrate (or cofactor) around its $K_m$ value while maintaining other components constant at the saturation levels. $K_{act}$ values for fumarate activation were obtained by fitting the saturation curves to the following equation:

$$v = v_0 + (V_{max} \cdot [\text{fumarate}])/(K_{act} + [\text{fumarate}]) \quad (1)$$

All calculations were carried out with the Sigma Plot 8.0 program (Jandel, San Rafael, CA).

**Table 1 Kinetic parameters for the WT and D102 mutant human m-NAD-MDHs**

Fumarate was added at 3 mM where indicated.

| Enzyme | Fumarate added | $K_{m,Malate}$ (mM) | $K_{m,Mg}$ (mM) | $K_{m,NAD}$ (mM) | $k_{cat}$ ($s^{-1}$) |
|---|---|---|---|---|---|
| WT (−) | No | 12.95 ± 2.46 | 3.53 ± 0.56 | 1.03 ± 0.04 | 130.50 ± 4.21 |
| WT (+) | Yes | 3.53 ± 0.16 | 0.90 ± 3.53 | 0.35 ± 0.02 | 206.40 ± 5.83 |
| D102E (−) | No | 13.01 ± 1.28 | 2.55 ± 0.39 | 0.80 ± 0.06 | 44.14 ± 1.23 |
| D102E (+) | Yes | 4.53 ± 0.21 | 0.91 ± 0.10 | 0.33 ± 0.03 | 60.61 ± 2.11 |
| D102A (−) | No | 9.12 ± 0.51 | 1.21 ± 0.10 | 0.40 ± 0.03 | 114.72 ± 5.95 |
| D102A (+) | Yes | 3.81 ± 0.34 | 0.47 ± 0.05 | 0.23 ± 0.04 | 127.14 ± 2.63 |
| D102K (−) | No | 7.86 ± 0.25 | 1.04 ± 0.09 | 0.44 ± 0.05 | 99.06 ± 0.59 |
| D102K (+) | Yes | 5.47 ± 0.30 | 0.53 ± 0.03 | 0.31 ± 0.04 | 111.09 ± 1.17 |

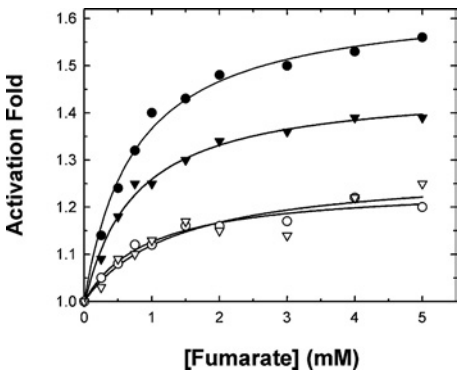


**Figure 2 Activation of human m-NAD-MDH by fumarate**

The assay mixture contained 15 mM malate, 10 mM $MgCl_2$ and 1 mM $NAD^+$. ●, WT enzyme; ▼, D102E; ○, D102A; ▽, D102K.

## RESULTS

### Kinetic properties of recombinant human m-NAD-MDH

The kinetic parameters for the WT (wild type) and mutant enzymes determined in the absence and presence of fumarate are shown in Table 1. There were no significant differences between the WT and mutant enzymes with regard to $K_m$ and $k_{cat}$ values; however, the extent of the decrease in $K_m$ and of the increase in $k_{cat}$ induced by fumarate was affected in the order: WT (D102) > D102E > D102A > D102K. The $K_m$ values of malate, $Mg^{2+}$ and $NAD^+$ for the WT enzyme were decreased 3–4-fold by fumarate, but for the D102K enzyme the $K_m$ values were reduced by only 1.5–2-fold.

### Correlation of fumarate activation with substrate concentration

The activating effects of fumarate on the WT and $Asp^{102}$ mutant enzymes were examined. When the enzymes were assayed under conditions of substrate concentrations around the $K_m$, the maximal activation by fumarate of the WT enzyme was approx. 1.6-fold, and that for the D102E enzyme was 1.4-fold. The other mutants, D102A and D102K, could be activated only slightly by fumarate (Figure 2). These preliminary results indicated that the anionic side chain of $Asp^{102}$ seems to have a significant effect on activation of the enzyme by fumarate.

To investigate further the relationship between activation by fumarate and substrate concentration, a wide range of substrate concentrations were used in the assay mixture. The activating effect of fumarate was more pronounced at lower substrate concentrations. Figure 3(A) shows the initial rate of the WT enzyme with or without fumarate at various malate concentrations. The fold activation was obtained by measuring the rate in the presence of fumarate ($v_t$) divided by each of the rates measured in the absence of fumarate ($v_0$). The activation of WT enzyme activity ranged from 14- to1.6-fold with increasing concentrations of malate (Figure 3B). Not only malate, but also $Mg^{2+}$ and $NAD^+$, had significant effects on activation by fumarate. The activation gradually disappeared with increasing malate, $Mg^{2+}$, or $NAD^+$ concentrations (Figures 3B, 3C and 3D respectively). The WT enzyme could be activated by 5–15-fold by low concentrations of malate, $Mg^{2+}$ and $NAD^+$, but the activation diminished when saturating concentrations were used.

Altering the charge properties of the side chain on residue 102 had a significant effect on activation of the enzyme by fumarate. The fumarate activation of the D102K mutant was much less sensitive to malate, $Mg^{2+}$ or $NAD^+$ concentration, and much lower *per se*. Similar phenomena were observed for D102A, but the activation of this mutant enzyme was slightly greater than for the D102K enzyme. The D102E mutant, in which the negative charge is preserved but the side chain is extended by one carbon, showed significantly decreased sensitivity to activation by fumarate compared with the WT enzyme. The activation of the D102E enzyme was slightly dependent on malate, $Mg^{2+}$ or $NAD^+$ concentration, but to a significantly lesser extent than that of the WT enzyme. The above results indicate that the allosteric regulation of m-NAD-MDH enzyme activity by fumarate is highly related to the active-site ligands, i.e. malate, $Mg^{2+}$ and $NAD^+$.

### Activation constants for WT and D102 mutant human m-NAD-MDHs

In order to delineate the mechanism of activation of m-NAD-MDH by fumarate, enzyme activities were assayed with a broad range of fumarate concentrations at different fixed concentrations of substrate (L-malate, $Mg^{2+}$ or $NAD^+$). Figure 4 shows the initial rates for the WT and D102 mutant enzymes with varying fumarate concentrations at each of the fixed malate concentrations. Similar concentration-dependent patterns were also observed for $Mg^{2+}$ and $NAD^+$ (results not shown). Each of the saturation curves plotted by the measured initial rates was fitted to eqn (1), and the activation constants ($K_{act}$) were obtained from these calculations.

The $K_{act,Fumarate}$ values were greatly dependent on the malate, $Mg^{2+}$ or $NAD^+$ concentration. $K_{act,Fumarate}$ decreased as the concentration of malate, $Mg^{2+}$ or $NAD^+$ increased. The $K_{act,Fumarate}$ value with respect to malate for the WT enzyme was 2.1 mM at the lowest malate concentration (25 $\mu$M) and fell gradually to a plateau value of 1.1 mM, indicating that the enzyme was activated by fumarate to the greatest extent at low malate concentrations, but decreased its requirement for fumarate upon elevating the malate concentration.

The dependence of $K_{act,Fumarate}$ on malate concentration for the D102E enzyme was similar to that of the WT enzyme, but the value was smaller than for the WT enzyme. The $K_{act,Fumarate}$ value for D102E was 1.4 mM at 25 $\mu$M malate, and fell steadily to a plateau value of 0.27 mM as the malate concentration increased, indicating that the catalytic activity of the D102E enzyme was significantly influenced by fumarate at low malate concentrations and that, similar to the WT enzyme, this mutant was activated less by fumarate as the malate concentration increased. However, the D102E enzyme had a lower requirement for fumarate than did the WT enzyme, since a lower $K_{act,Fumarate}$ was observed for this mutant, suggesting that the allosteric regulation of the D102E enzyme by fumarate is somewhat impaired.

The enzyme activities of D102A and D102K were not stimulated by fumarate (Figure 2), in agreement with the small and constant $K_{act,Fumarate}$ values of these mutants compared with those

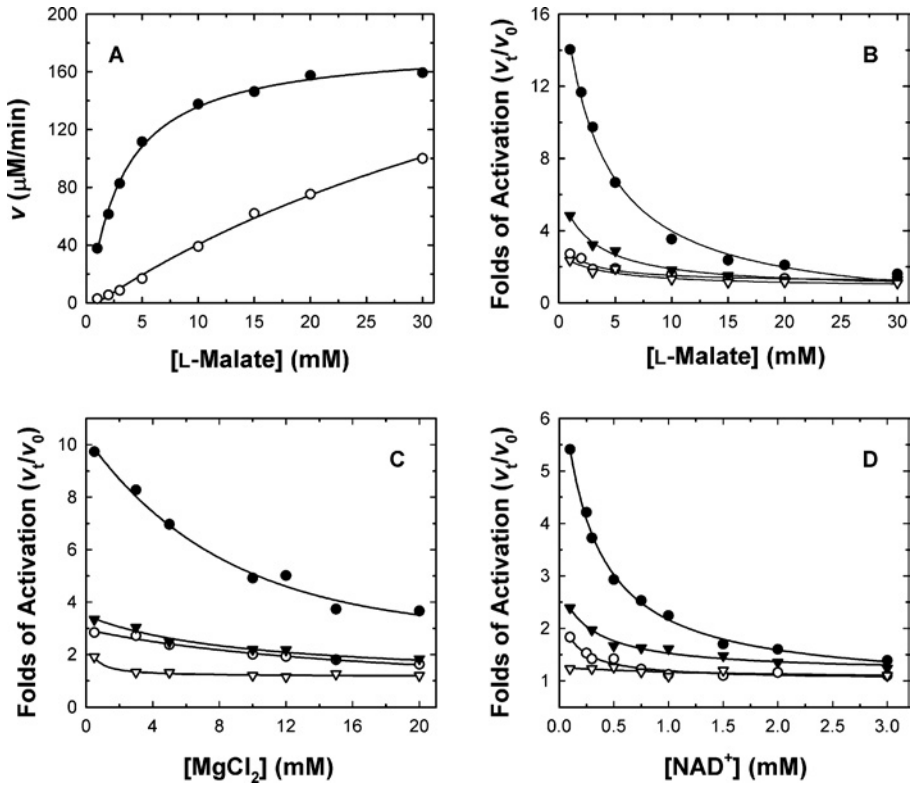


**Figure 3 Substrate and cofactor concentration-dependence of the activation of human m-NAD-MDH by fumarate**

The fumarate concentration was fixed at 3 mM to achieve maximal activation of the enzyme under the indicated conditions. (**A**) Initial rate of the WT enzyme with (●; $v_t$) or without (○; $v_0$) 3 mM fumarate at various malate concentrations. The concentrations of $MgCl_2$ and $NAD^+$ were fixed at 10 mM and 1.0 mM respectively. In (**B**)–(**D**), each point was obtained from $v_t$ divided by $v_0$ at various concentrations of malate, $MgCl_2$ and $NAD^+$ respectively. The non-varied substrate concentrations in (**B**)–(**D**) were 15, 10 and 1.0 mM for L-malate, $MgCl_2$ and $NAD^+$ respectively. ●, WT enzyme; ▼, D102E; ○, D102A; ▽, D102K.

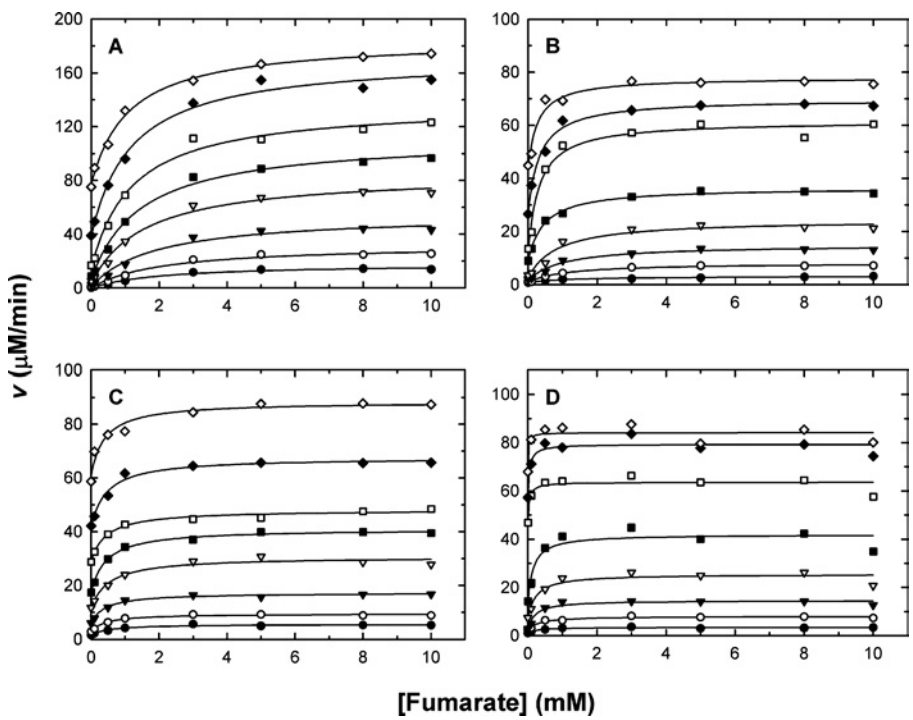


**Figure 4 Activation by fumarate of human m-NAD-MDH at various malate concentrations**

The initial velocities were measured at 50 mM Tris/HCl (pH 7.4), 10 mM $MgCl_2$ and 1.0 mM $NAD^+$. The malate concentrations used were, from top to bottom, 0.25, 0.5, 1, 2, 3, 5, 10 and 15 mM. (**A**) WT; (**B**) D102E; (**C**) D102A; (**D**) D102K.

of the WT and D102E enzymes. The $K_{act,Fumarate}$ values of these two mutant enzymes in the presence of a broad range of malate concentrations were 0.52–0.39 and 0.23–0.01 mM respectively. The malate-concentration-independence of $K_{act,Fumarate}$ for the D102A and D102K enzymes indicated that mutation of this residue to one with a neutral or positively charged side chain significantly diminished allosteric activation by fumarate.

The effects of the concentrations of $Mg^{2+}$ and $NAD^+$ on $K_{act,Fumarate}$ for the WT and D102E enzyme were similar to those of malate. For the WT enzyme, the $K_{act,Fumarate}$ value with respect to $Mg^{2+}$ fell from 5.1 mM at the lowest $Mg^{2+}$ concentration (0.5 mM) to a plateau value of 1.2 mM; that for $NAD^+$ fell from 2.2 mM to 0.6 mM. For the D102E enzyme, the $K_{act,Fumarate}$ value with respect to $Mg^{2+}$ fell from 2.6 mM to a plateau value of 1.2 mM; that for $NAD^+$ fell from 1.5 mM to 0.6 mM. For the other two mutant enzymes, D102A and D102K, $K_{act,Fumarate}$ was almost independent of both $Mg^{2+}$ and $NAD^+$ concentrations, indicating the significance of the regulatory role of $Asp^{102}$ for activation by fumarate. Among the WT and mutant enzymes, the $K_{act,Fumarate}$ value of D102K showed a minimum dependence on all three ligands, implying that the balance of electrostatic interactions is essential for allosteric regulation by fumarate.

### Apparent $K_m$ values on activation by fumarate

Fumarate decreased the apparent $K_m$ values for malate, $Mg^{2+}$ and $NAD^+$ of the recombinant WT and D102 mutant enzymes (Table 1). We examined the dependence of $K_m$ on fumarate concentration in the range 0–10 mM for the WT and D102 mutant enzymes. The apparent $K_{m,Malate}$ for the WT enzyme was 12.95 mM without fumarate, and it fell gradually to a plateau value of 4.41 mM at a saturating fumarate concentration. The apparent $K_{m,Mg}$ and $K_{m,NAD}$ values were 3.53 and 1.03 mM without fumarate, falling to plateau values of 0.69 and 0.22 mM respectively. The apparent value of $K_{m,Malate}$ was reduced by 2.9-fold, that of $K_{m,Mg}$ was reduced by 5.1-fold, and that of $K_{m,NAD}$ was reduced by 4.7-fold, indicating that activation of the enzyme by fumarate was due to the enhancement of the affinity of the enzyme for its ligands (malate, $Mg^{2+}$ and $NAD^+$) at the active site. The mutant enzymes showed a slightly smaller decrease in apparent $K_m$ values compared with the WT enzyme. For the D102E enzyme, the values of apparent $K_{m,Malate}$ and $K_{m,Mg}$ were reduced by 2.3-fold (13.01 to 5.60 mM) and 4.3-fold (2.55 to 0.59 mM) respectively, similar to the WT enzyme. The $K_{m,NAD}$ value of the D102E enzyme was reduced by only 2-fold (0.80 to 0.45 mM), less than the decrease observed for the WT enzyme (4.7-fold). For the D102A enzyme, the apparent $K_m$ values were reduced by only approx. 2-fold. The apparent $K_{m,Malate}$, $K_{m,Mg}$ and $K_{m,NAD}$ values were 9.12, 1.21 and 0.40 mM respectively without fumarate, and decreased steadily to plateau values of 4.53, 0.50 and 0.21 mM respectively. For the D102K enzyme, the apparent $K_m$ values for malate and $NAD^+$ were not changed significantly in the presence of fumarate. The apparent $K_{m,Malate}$ values were 7.86 and 6.87 mM, and $K_{m,NAD}$ values were 0.44 and 0.33 mM, without and with 10 mM fumarate respectively. The $K_{m,Mg}$ of the D102K enzyme was reduced by 1.9-fold (1.04 to 0.54 mM), similar to that of the D102A enzyme.

## DISCUSSION

### Binding site for the allosteric activator fumarate

Earlier studies have suggested that fumarate is an allosteric activator of human m-NAD-MDH, by decreasing the $K_m$ of malate [19,28]. The catalytic activity of *A. suum* m-NAD-MDH is also activated by fumarate [23,24]. The crystal structure of human m-NAD-MDH complexed with fumarate has been resolved, and the mode of binding of fumarate in human m-NAD-MDH has been identified [20]. The allosteric regulation of human m-NAD-MDH by fumarate is consistent with its role in glutamine metabolism for energy production, since fumarate is the product of the preceding step of this pathway [6]. The c-NADP-MDH isoform, which is involved in the generation of NADPH for fatty acid synthesis, is therefore not subject to regulation by fumarate.

Two arginine residues in the fumarate binding pocket, $Arg^{67}$ and $Arg^{91}$, have been identified as being essential for the binding of fumarate to the enzyme (Figure 1B). However, both $Arg^{67}$ and $Arg^{91}$ are conserved in many other decarboxylating MDHs (Figure 5A) that cannot be activated by fumarate. $Glu^{59}$, which is ion-paired with $Arg^{67}$ in the structure but is not conserved among the MDHs, has a profound influence on activation by fumarate: mutation of this residue made the enzyme completely insensitive to fumarate [20]. These results prompted us to look for additional factors governing activation by fumarate. According to the crystal structure, the fumarate binding pocket is highly hydrophilic [20], and there are many charged residues in this binding site (Figure 5B). We chose $Asp^{102}$ because it is present only in the human and *A. suum* m-NAD-MDHs, but not in other decarboxylating MDHs (Figure 5A). Figure 5(B) shows that $Asp^{102}$ is close to the $Arg^{67}$–fumarate–$Arg^{91}$ ion-pair network. Our kinetic data clearly demonstrate that $Asp^{102}$ is an important amino acid for activation of the enzyme by fumarate. We verify that the negative charge of the side chain in $Asp^{102}$ is involved in this activation. Altering the charge properties of this residue has a substantial impact on activation by fumarate (Figure 2) and sensitivity of the enzyme to substrates (Figure 3). Our experimental results suggest that the negative charge of $Asp^{102}$ is crucial for activation by fumarate. Retaining the negative charge in the D102E enzyme conserved approx. 80–90 % of the activation capacity of the WT enzyme (Figure 2), but activation was less sensitive to substrates. $Asp^{102}$ may be ion-paired with another positively charged amino acid residue. Changing the length of the side chain may impede this ionic interaction, thus interfering with the electrostatic balance in this allosteric site that is crucial for fumarate activation.

The $K_{act}$ values of the WT enzyme decrease upon increasing the concentration of substrate (malate, $Mg^{2+}$ or $NAD^+$), indicating that the binding of fumarate and substrates is synergistic in order to optimize the catalytic machinery of the enzyme. Mutation of $Asp^{102}$, however, desensitizes this co-operative effect (Figure 3). This result is corroborated by the allosteric binding of fumarate, since competition for the same binding site by fumarate and substrates would bring about an increase in the apparent $K_{act}$ value. Thus fumarate may bind to the active centre as well, albeit with low affinity, and a high fumarate concentration (above 20 mM fumarate) inhibits enzyme activation (results not shown).

### Significance of $Asp^{102}$ in the fumarate binding site

Structural data have clearly revealed that human m-NAD-MDH without any active-site ligands (open form I) is not compatible with fumarate binding, since the side chain of $Phe^{68}$ assumes a different conformation to block this binding site, and the guanidinium group of $Arg^{91}$ is rotated away from the binding site [20]. Substrate binding (malate, $Mg^{2+}$ and $NAD^+$) induces a transition of the enzyme from open form I to closed form I, which is catalytically active to execute the chemical reaction. Open form II, in which fumarate is bound, may have a higher affinity for the substrates, since the $K_m$ values of the WT enzyme decrease as the fumarate concentration increases, demonstrating that binding of fumarate at the allosteric site enhances the binding of substrates at the active site, and thus the maximal activity of the enzyme can

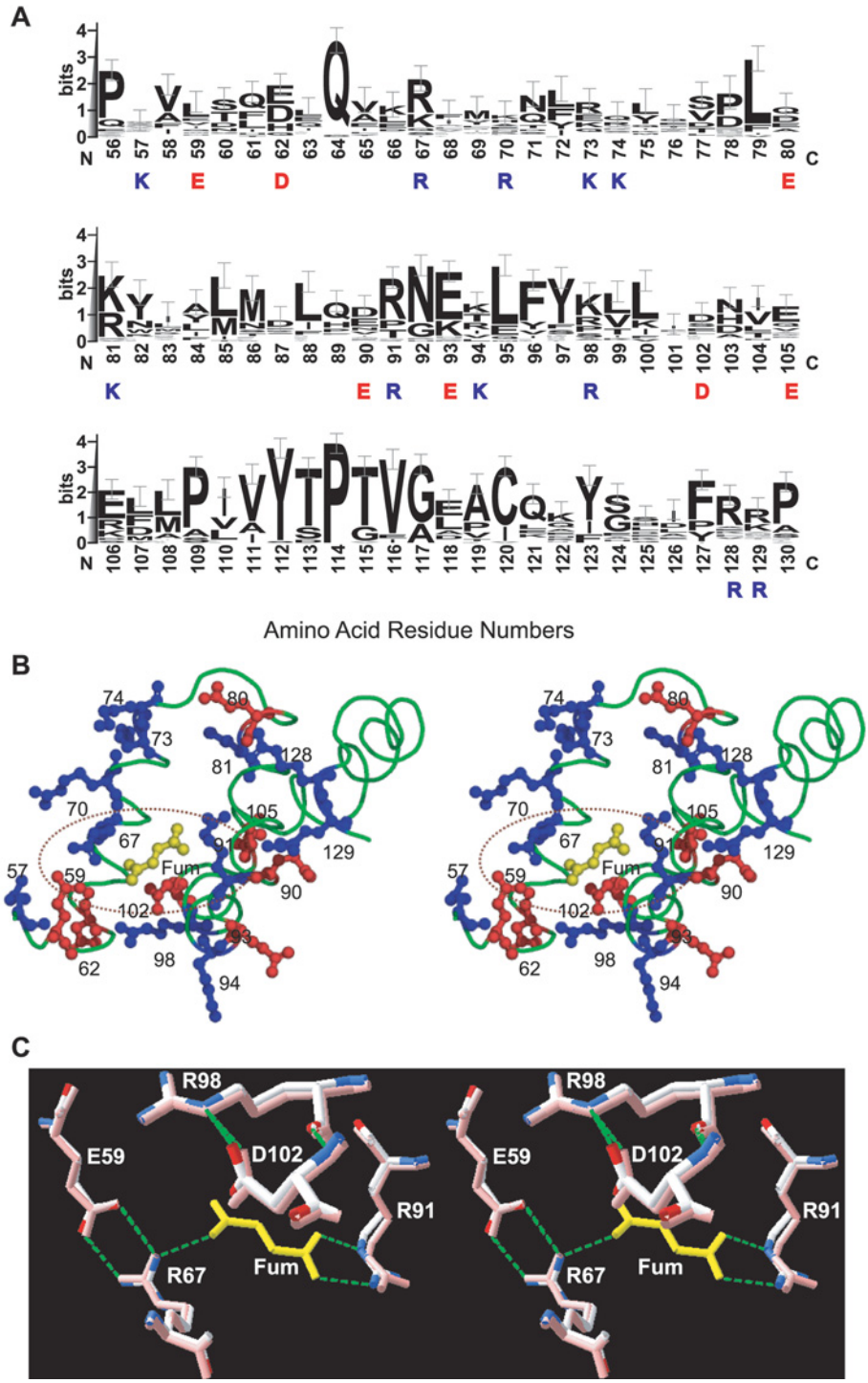


**Figure 5 Fumarate binding region of human m-NAD-MDH**

(**A**) Sequence alignments around the fumarate binding site of the 35 decarboxylating MDHs with amino acid sequences available. Amino acid sequences of the enzymes were searched by Blast [30] and alignments were generated by Clustal W [31]. The results are expressed by sequence logos with error bars [32]. The amino acid residues highlighted are charged residues in the fumarate binding region; blue for positively and red for negatively charged amino acids. (**B**) Local structural representation of the charged amino acid residues at the fumarate (Fum) binding region. Blue indicates basic residues (Lys and Arg) and red indicates acidic residues (Asp and Glu). This figure was generated with PyMOL (DeLano Scientific LLC). (**C**) Superimposition of the closed form I (PDB code 1do8; in pink) and closed form II (PDB code 1pj4) structures, indicating the location and conformation of $Asp^{102}$ in the fumarate binding pocket. The green dashed lines representing hydrogen bonds between amino acid residues and fumarate (in yellow) were generated by Swiss-Pdb Viewer [33].

be achieved. On the other hand, closed form I (substrates bound) could be converted into closed form II after binding of fumarate to the enzyme [10]. However, the requirement for fumarate for this transition becomes negligible at high substrate concentrations. In agreement with this, activation was up to 10-fold at the lowest substrate concentrations, but was only 1.5-fold when saturating

substrate was present (Figure 3), and decreases in the $K_{act}$ values of the enzyme were observed as the concentration of substrate was elevated.

Figure 5(C) shows the superimposition of the fumarate binding pocket of closed form I (PDB code 1do8), which is bound with active-site ligands only, and closed form II (PDB code 1pj4), which is bound with active-site ligands and the allosteric ligand fumarate. In closed form I, even without a fumarate molecule, the allosteric site is available for fumarate binding; the side chains of $Arg^{67}$ and $Arg^{91}$, which are the fumarate binding ligands, display almost the same conformations as observed in closed form II. $Asp^{102}$ is in close proximity to the $Arg^{67}$–fumarate–$Arg^{91}$ ion-pair network, and its side-chain conformation is the same in closed forms I and II. $Asp^{102}$ does not interact directly with fumarate, and is hydrogen-bonded and may be ion-paired with $Arg^{98}$. From our kinetic data, we suggest that the role of $Asp^{102}$ is to maintain the electrostatic balance in the fumarate binding pocket. Mutation of $Asp^{102}$ to Ala and Lys, however, abolishes the allosteric regulation of the enzyme. $Asp^{102}$ is not conserved in all the enzymes. In pigeon c-NADP-MDH, which is not allosterically activated by fumarate, the corresponding amino acid residue 102 is Ser, which has a neutral side chain.

## Conclusions

In summary, fumarate enhances the binding affinity of m-NAD-MDH for its ligands at the active site, since it decreases the apparent $K_m$ values of malate, $Mg^{2+}$ and $NAD^+$. The susceptibility of substrate $K_m$ values to allosteric activation is partially conserved in the D102E enzyme, but almost abolished in the D102A and D102K enzymes, suggesting that mutation of $Asp^{102}$ causes the enzyme to be non-allosterically regulated by fumarate. The significance of $Asp^{102}$ in the fumarate binding site is in the maintenance of the electrostatic balance that may be a critical factor governing the mechanism of regulation by fumarate.

This work was supported by the National Science Council, ROC (grants NSC 91-2320-B-005-004 and NSC-93-2311-B-005-018 to H.-C. H.).

## REFERENCES


1 Frenkel, R. (1975) Regulation and physiological function of malic enzyme. Curr. Top. Cell. Regul. **9**, 157–181
2 Hsu, R. Y. (1982) Pigeon liver malic enzyme. Mol. Cell. Biochem. **43**, 3–26
3 Loeber, G., Infante, A. A., Maurer-Fogy, I., Krystek, E. and Dworkin, M. B. (1991) Human $NAD^+$-dependent mitochondrial malic enzyme. J. Biol. Chem. **266**, 3016–3021
4 Rao, G. S. J., Coleman, D. E., Kulkarni, G., Goldsmith, E. J., Cook, P. F. and Harris, B. G. (2000) NAD-malic enzyme from Ascaris suum: sequence and structural studies. Protein Pept. Lett. **7**, 297–304
5 Cleland, W. W. (2000) Chemical mechanism of malic enzyme as determined by isotope effects and alternate substrates. Protein Pept. Lett. **7**, 305–312
6 Xu, Y., Bhargava, G., Wu, H., Loeber, G. and Tong, L. (1999) Crystal structure of human mitochondrial $NAD(P)^+$-dependent malic enzyme: a new class of oxidative decarboxylases. Structure **7**, 877–889
7 Yang, Z., Floyd, D. L., Loeber, G. and Tong, L. (2000) Structure of a closed form of human malic enzyme and implications for catalytic mechanism. Nat. Struct. Biol. **7**, 251–257
8 Yang, Z., Zhang, H., Hung, H. C., Kuo, C. C., Tsai, L. C., Yuan, H. S., Chou, W. Y., Chang, G. G. and Tong, L. (2002) Structural studies of the pigeon cytosolic $NADP^+$-dependent malic enzyme. Protein Sci. **11**, 332–341
9 Coleman, D. E., Rao, G. S., Goldsmith, E. J., Cook, P. F. and Harris, B. G. (2002) Crystal structure of the malic enzyme from Ascaris suum complexed with nicotinamide adenine dinucleotide at 2.3 Å resolution. Biochemistry **41**, 6928–6938
10 Chang, G. G. and Tong, L. (2003) Structure and function of malic enzymes, a new class of oxidative decarboxylases. Biochemistry **42**, 12721–12733
11 Loeber, G., Dworkin, M. B., Infante, A. and Ahorn, H. (1994) Characterization of cytosolic malic enzyme in human tumor cells. FEBS Lett. **344**, 181–186
12 Sauer, L. A., Dauchy, R. T., Nagel, W. O. and Morris, H. P. (1980) Mitochondrial malic enzymes. Mitochondrial $NAD(P)^+$-dependent malic enzyme activity and malate-dependent pyruvate formation are progression-linked in Morris hepatomas. J. Biol. Chem. **255**, 3844–3848
13 Baggetto, L. G. (1992) Deviant energetic metabolism of glycolytic cancer cells. Biochimie **74**, 959–974
14 Sanz, N., Diez-Fernandez, D., Valverde, A. M., Lorenzo, M., Benito, M. and Cascales, M. (1997) Malic enzyme and glucose 6-phosphate dehydrogenase gene expression increases in rat liver cirrhogenesis. Br. J. Cancer **75**, 487–492
15 Moreadith, R. W. and Lehninger, A. L. (1984) The pathways of glutamate and glutamine oxidation by tumor cell mitochondria. Role of mitochondrial $NAD(P)^+$-dependent malic enzyme. J. Biol. Chem. **259**, 6215–6221
16 Moreadith, R. W. and Lehninger, A. L. (1984) Purification, kinetic behavior, and regulation of $NAD(P)^+$ malic enzyme of tumor mitochondria. J. Biol. Chem. **259**, 6222–6227
17 Fahien, L. A. and Teller, J. K. (1992) Glutamate-malate metabolism in liver mitochondria. J. Biol. Chem. **267**, 10411–10422
18 Teller, J. K., Fahien, L. A. and Davis, J. W. (1992) Kinetic and regulation of hepatoma mitochondrial NAD(P) malic enzyme. J. Biol. Chem. **267**, 10423–10432
19 Sauer, L. A. (1973) An NAD- and NADP-dependent malic enzyme with regulatory properties in rat liver and adrenal cortex mitochondrial fractions. Biochem. Biophys. Res. Commun. **50**, 524–531
20 Yang, Z., Lanks, C. W. and Tong, L. (2002) Molecular mechanism for the regulation of human mitochondrial $NAD(P)^+$-dependent malic enzyme by ATP and fumarate. Structure **10**, 951–960
21 Rao, G. S. J., Coleman, D. E., Karsten, W. E., Cook, P. F. and Harris, B. G. (2003) Crystallographic studies on Ascaris suum NAD-malic enzyme bound to reduced cofactor and identification of an effector site. J. Biol. Chem. **278**, 38051–38058
22 Tao, X., Yang, Z. and Tong, L. (2003) Crystal structures of substrate complexes of malic enzyme and insights into the catalytic mechanism. Structure **11**, 1141–1150
23 Landsperger, W. J. and Harris, B. G. (1976) NAD+-malic enzyme. Regulatory properties of the enzyme from Ascaris suum. J. Biol. Chem. **251**, 3599–3602
24 Lai, C. J., Harris, B. G. and Cook, P. F. (1992) Mechanism of activation of the NAD-malic enzyme from Ascaris suum by fumarate. Arch. Biochem. Biophys. **299**, 214–219
25 Karsten, W. E., Pais, J. E., Rao, G. S., Harris, B. G. and Cook, P. F. (2003) Ascaris suum NAD-malic enzyme is activated by L-malate and fumarate binding to separate allosteric site. Biochemistry **42**, 9712–9721
26 Bhargava, G., Mui, S., Pav, S., Wu, H., Loeber, G. and Tong, L. (1999) Preliminary crystallographic studies of human mitochondrial NAD(P)(+)-dependent malic enzyme. J. Struct. Biol. **127**, 72–75
27 Bradford, M. M. (1976) A rapid and sensitive method for the quantitation of microgram quantities of protein, utilizing the principle of protein-dye binding. Anal. Biochem. **72**, 248–254
28 Mandella, R. D. and Sauer, L. A. T. (1975) The mitochondrial malic enzymes I. Submitochondrial localization and purification and properties of the $NAD(P)^+$-dependent enzyme from adrenal cortex. J. Biol. Chem. **250**, 5877–5884
29 Wallace, A. C., Laskowski, R. A. and Thornton, J. M. (1995) LIGPLOT: A program to generate schematic diagrams of protein-ligand interactions. Proten Eng. **8**, 127–134
30 Altschul, S. F., Boguski, M. S., Gish, W. and Wootton, J. C. (1994) Issues in searching molecular sequence databases. Nat. Genet. **6**, 119–129
31 Higgins, D., Thompson, J., Gibson, T., Thompson, J. D., Higgins, D. G. and Gibson, T. J. (1994) CLUSTAL W: improving the sensitivity of progressive multiple sequence alignment through sequence weighting, position-specific gap penalties and weight matrix choice. Nucleic Acids Res. **22**, 4673–4680
32 Crooks, G. E., Hon, G., Chandonia, J. M. and Brenner, S. E. (2004) WebLogo: A sequence logo generator. Genome Res. **14**, 1188–1190
33 Guex, N. and Peitsch, M. C. (1997) SWISS-MODEL and the Swiss-Pdb Viewer: An environment for comparative protein modeling. Electrophoresis **18**, 2714–2723


Received 20 April 2005/20 June 2005; accepted 30 June 2005
Published as BJ Immediate Publication 30 June 2005, doi:10.1042/BJ20050641